Int. J. Solids Structures Vol. 26, No. 5 6, pp. 499–510, 1990
Printed in Great Britain.

0020–7683/90 $3.00 + .00

ON THE PREDICTION OF INTERLAMINAR SHEAR STRESSES IN A THICK LAMINATED GENERAL SHELL

REAZ A. CHAUDHURI
Department of Civil Engineering, University of Utah, Salt Lake City, UT 84112, U.S.A.

(*Received* 13 *January* 1988; *in revised form* 8 *February* 1989)

Abstract—A post-processing semi-analytical approach, for prediction of the interlaminar shear stress distribution through the thickness of an arbitrarily laminated general shell, is presented. The starting point of the approach is an assumed displacement finite element analysis, based on the assumptions of transverse inextensibility and layerwise constant shear-angle theory (LCST). First, the problem is posed in the context of Taylor series expansions of the interlaminar shear stresses in terms of the thickness coordinate, dictated by the LCST assumption and the shell curvature. An "exact" (in the context of the problem thus posed) and three progressively approximate semi-analytical methods for prediction of interlaminar shear stresses are then presented. The through-thickness distribution of interlaminar shear stresses in an arbitrarily laminated thick plate can be obtained as a special case of the present solution. Numerical results are presented for two-layer thin and thick tubes with simply-supported edges, using the Cartesian-like local Riemann coordinate (CLRC) approximation and are compared to the corresponding analytical solutions, based on the classical lamination theory (CLT). Results for thin laminated tubes prove the accuracy of the present approach, while hitherto unavailable results for a thick laminated tube are expected to serve as baseline solutions for future comparisons.

NOMENCLATURE

$\mathbf{a}_r$	fixed natural coordinates basis vectors
$\{d_j^{(i)}\}$	nodal displacement vector for the jth layer-element belonging to the ith layer
E_{ij}	Young's moduli of an anisotropic layer-material, $i, j = 1, 2$
G_{ij}	shear moduli of an anisotropic layer-material, $i, j \neq 1, 2, 3$
$\mathbf{g}_m$	tangent (to the α-, β-, ζ-curves) vectors
g_{mn}	metric tensor
g^{mn}	associated metric tensor
$\bar{g}_\alpha, \bar{g}_\beta$	first fundamental quantities of the shell reference surface for lines of curvature coordinates
$\mathbf{i}_r$	orthogonal basis vectors for fixed Cartesian coordinates
L	length of a cylindrical shell
N	total number of layers
$\bar{n}_r$	rth physical component of the unit normal vector
p_i	uniform pressure acting on the inner surface of a cylindrical shell
Q_{ij}	reduced elastic stiffness of an anisotropic layer-material
$\bar{Q}_{ij}$	reduced elastic stiffness of an orthotropic layer-material
R	inner radius of a cylindrical shell
R_{ij}	reduced elastic compliance of an anisotropic layer-material
$1/R_\alpha, 1/R_\beta$	principal normal curvatures of the shell reference surface
$1/R_\Gamma, 1/R_n, 1/R_{n\Gamma}$	normal curvatures and twist of the shell reference surface with respect to the directions parallel and normal to the boundary curve
$\bar{s}$	area measured on the shell reference surface
$\bar{s}_j$	area of the jth layer-element belonging to the ith layer, measured on the shell reference surface
t	total thickness of the shell wall
t_i	thickness of the ith layer, $i = 1, \ldots, N$
x, y	Cartesian-like local Riemann coordinates in the directions of the lines of curvature α and β, respectively
z, ζ	transverse coordinate direction
x, θ, z (or ζ)	circular cylindrical shell coordinates
α, β	lines of curvature coordinates measured on the shell reference surface
Γ	direction tangential to the boundary curve; also curved length measured on the boundary curve
Γ^m_{ip}	Euclidean–Christoffel symbol
$\gamma^{(i)}_{\alpha\zeta}, \gamma^{(i)}_{\beta\zeta}$	covariant components of the interlaminar strains at a point inside the ith layer
$\varepsilon^{(i)}_\alpha(\zeta), \varepsilon^{(i)}_\beta(\zeta), \varepsilon^{(i)}_{\alpha\beta}(\zeta)$	surface parallel components of strain at a point inside the ith layer
$\varepsilon^{(i)}_{\alpha\zeta}(\zeta), \varepsilon^{(i)}_{\beta\zeta}(\zeta)$	transverse (interlaminar) shear strains at a point inside the ith layer
θ_i	fiber orientation in the ith layer, measured with respect to the α-direction

ν_{ij}	Poisson's ratios, $i \neq j$
$\sigma_x^{(i)}(\zeta), \sigma_\beta^{(i)}(\zeta), \sigma_{x\beta}^{(i)}(\zeta)$	surface-parallel components of stress at a point inside the ith layer
$\sigma_{x\zeta}^{(i)}(\zeta), \sigma_{\beta\zeta}^{(i)}(\zeta)$	transverse (interlaminar) shear stresses at a point inside the ith layer
τ^{lm}	contravariant components of the stress tensor
$\{\phi\}_i$	vector of shape functions of a triangular layer-element
ϕ	angle between the tangent to the boundary curve Γ and the x-direction.

1. INTRODUCTION

Failure analysis of thick-section fiber reinforced laminated shells necessitates accurate prediction of the interlaminar (transverse) shear stresses, because of the role they play in causing delamination and shear crippling failures, especially in the vicinity of ply-drops, edges or other discontinuities. Analytical solutions are relatively scarce and are primarily restricted to one or more of the following: simple shell geometry (e.g. cylindrical and spherical shells), shallow-shell approximation, thin (Love–Kirchhoff hypothesis) or moderately thick (Reissner–Mindlin hypothesis) shell theory, cross-ply lamination, special boundary conditions (e.g. SS3 under the classification of Hoff and Rehfield, 1965), simple loading conditions, and so forth. A numerical procedure, such as the finite element method (FEM), appears to be the only practical alternative because of the ease with which problems of arbitrary shell geometry, irregular shapes, non-uniform thickness, anisotropy, arbitrary lamination, arbitrary boundary conditions, and general loadings can be handled by this method. A review of the FEM literature, however, suggests that, short of performing a highly refined three-dimensional analysis, few FEM-based methods are available which can predict the accurate interlaminar shear stress distribution through the thickness of a general laminated shell.

Recently, Chaudhuri (1983) and Seide and Chaudhuri (1987) have developed an assumed-quadratic- (in the curvilinear coordinate plane) displacement-potential-energy-approach-based laminated general shell element of triangular planform, the kinematic relations being derived under the general assumptions of transverse inextensibility and layerwise constant shear-angle theory (LCST). Once the nodal displacements are computed, the element stresses can be easily obtained [see eqn (1) of Chaudhuri and Seide, 1987a]. It is noteworthy that while accurate surface-parallel components of stresses can be computed at special points on the interface triangle, the interlaminar shear stress components, $\bar{\sigma}_{x\zeta}^{(i)}(\zeta)$ and $\bar{\sigma}_{\beta\zeta}^{(i)}(\zeta)$ thus obtained, do not represent the true interlaminar shear stresses. They are essentially the physical components of the interlaminar shear stresses corresponding to the through-thickness-average covariant components of the true interlaminar shear strains [the same is true for $\bar{\varepsilon}_{x\zeta}^{(i)}(\zeta)$ and $\bar{\varepsilon}_{\beta\zeta}^{(i)}(\zeta)$]. The primary objective of the present study is to develop a semi-analytical approach for prediction of interlaminar shear stress distribution through the thickness of an arbitrary laminated general shell. A recent study by Chaudhuri and Seide (1987b) has presented a semi-analytical approach for prediction of interlaminar shear stress distribution through the thickness of an arbitrarily laminated thick anisotropic plate. Extension of the concept presented there to the case of an arbitrarily laminated thick general shell is a challenge yet to be undertaken. The many-fold complexity of the analysis of the deformation of a solid body in the general Riemannian space, in comparison to the same in the Euclidean space, renders the extension of the approach outlined in the above study to the case of an arbitrarily laminated general shell an extremely difficult task. This difficulty is primarily mathematical in nature and approximations, based on sound physical judgements, must be employed to obtain a reasonably accurate solution to the problem under investigation, because derivation of an exact solution to the problem appears to be a synonym of impossibility at the present moment.

2. FORMULATION OF THE PROBLEM

Equations of equilibrium for a general shell neglecting the body forces are given by

$$\tau^{lm}/l = 0 \quad \text{for} \quad m, l = 1 \text{ (or } x\text{)}, 2 \text{ (or } \beta\text{)}, 3 \text{ (or } z\text{)} \tag{1}$$

where the covariant derivatives of contravariant components of stresses, τ^{lm}, are defined as

$$\tau^{lm}/l = \tau^{lm}_{,l} + \Gamma^{m}_{lp}\tau^{lp} + \Gamma^{p}_{lp}\tau^{lm} \tag{2}$$

while the Euclidean–Christoffel symbol, Γ^{m}_{lp}, is defined as

$$\Gamma^{m}_{lp} = \tfrac{1}{2}g^{mn}(g_{np,l} + g_{ln,p} - g_{lp,n}) = \Gamma^{m}_{pl} \tag{3}$$

with

$$g_{11}(z) = \frac{1}{g^{11}(z)} = \bar{g}_{11}(1 + z/R_\alpha)^2 \tag{4a}$$

$$g_{22}(z) = \frac{1}{g^{22}(z)} = \bar{g}_{22}(1 + z/R_\beta)^2 \tag{4b}$$

$$g_{33}(z) = 1/g^{33}(z) = 1 \tag{4c}$$

$$g_{mn}(z) = g^{mn}(z) = 0 \quad \text{for} \quad m \neq n. \tag{4d}$$

The relations (4) hold on account of selection of the orthogonal curvilinear coordinate system α, β, z where α and β denote the directions of the lines of curvature of the shell reference (bottom) surface, while z denotes the direction of the normal to the reference surface. It is noteworthy that α, β and z represent the local (or element) coordinates for the N-layer composite element. For a layer element, ζ denotes the direction of the normal and is given by

$$z = \bar{d}_i + \zeta \tag{5a}$$

where

$$\bar{d}_i = \sum_{m=1}^{i-1} t_m; \quad \bar{d}_1 = 0. \tag{5b}$$

Substitution of eqns (2)–(5) into eqn (1), with $m = 1$ (or α), will lead to the first equation of equilibrium in terms of the physical components of the stresses

$$\begin{aligned}
&\frac{\partial}{\partial\zeta}\left[\left(1+\frac{\bar{d}_i+\zeta}{R_\alpha}\right)^2\left(1+\frac{\bar{d}_i+\zeta}{R_\beta}\right)\sigma^{(i)}_{\alpha\zeta}(\zeta)\right] \\
&\quad = -\frac{1}{\bar{g}_\alpha\bar{g}_\beta}\left\{\frac{1}{\bar{g}_\alpha}\frac{\partial}{\partial\beta}\left[\bar{g}_\alpha^2\left(1+\frac{\bar{d}_i+\zeta}{R_\alpha}\right)^2\sigma^{(i)}_{\alpha\beta}(\zeta)\right]\right. \\
&\qquad + \bar{g}_\beta\left(1+\frac{\bar{d}_i+\zeta}{R_\alpha}\right)\left(1+\frac{\bar{d}_i+\zeta}{R_\beta}\right)\frac{\partial\sigma^{(i)}_\alpha(\zeta)}{\partial\alpha} \\
&\qquad \left. + \frac{\partial\bar{g}_\beta}{\partial\alpha}\left(1+\frac{\bar{d}_i+\zeta}{R_\alpha}\right)^2[\sigma^{(i)}_\alpha(\zeta) - \sigma^{(i)}_\beta(\zeta)]\right\}
\end{aligned} \tag{6a}$$

where

$$\bar{g}_\alpha = (\bar{g}_{11})^{1/2}, \quad \bar{g}_\beta = (\bar{g}_{22})^{1/2}. \tag{6b}$$

The second equation of equilibrium of elasticity can be obtained from eqn (6a) by replacing α by β and vice versa.

In the case of a laminated plate, $g_\alpha = g_\beta = 1$, $R_\alpha = R_\beta = \infty$. Equation (6a), in view of the assumptions of the LCST, then reduces to

$$\sigma_{\alpha\zeta}^{(i)}(\zeta) = A_1^{(i)}(x_1, x_2) + A_2^{(i)}(x_1, x_2)\zeta + A_3^{(i)}(x_1, x_2)\zeta^2 \tag{7}$$

where x_1, x_2 are rectangular Cartesian coordinates.

In the case of a laminated shell, because of the effect of the curvature, the expression for $\sigma_{\alpha\zeta}^{(i)}(\zeta)$ [and $\sigma_{\beta\zeta}^{(i)}(\zeta)$] will be comprised of more complicated functions of ζ, even when the surface-parallel displacements are assumed to vary linearly through the thickness of a layer (LCST). Nonetheless, since they are expected to be regular functions of ζ, in the range $0 \leqslant \zeta \leqslant t_i$, they can be assumed to be in the form of a power series (essentially a Taylor series expansion). Inclusion of the curvature effect into the formulation, however, demands that a power series of order at least three be assumed:

$$\sigma_{r\zeta}^{(i)}(\zeta) = \sum_{m=0}^{n} B_{rm}^{(i)}\zeta^m \quad \text{for} \quad r = \alpha, \beta;\ n \geqslant 3. \tag{8}$$

Prediction of $\sigma_{rz}(z), r = \alpha, \beta$, through the thickness of an N-layer laminated general shell necessitates the determination of $2N(n+1)$ unknown coefficients, which, in turn, ask for as many conditions or equations to be supplied by the physics of the problem.

Equation (8) can be expressed in the alternate form

$$\sigma_{r\zeta}^{(i)}(\zeta) = \sum_{m=1}^{n+1} \bar{f}_{rm}^{(i)} H_m(\zeta) \quad \text{for} \quad r = \alpha, \beta \tag{9}$$

where $H_m(\zeta)$ are the one-dimensional shape functions or Lagrangian interpolation functions (Zienkiewicz, 1977). $\bar{f}_{rm}^{(i)}$ are the magnitudes of $\sigma_{r\zeta}^{(i)}(\zeta)$ at the $n+1$ points. Here ζ_m, $m = 1, \ldots, n+1$. $\zeta_1 = 0$; $\zeta_{n+1} = t_i$ and ζ_m, $m = 2, \ldots, n$ may be conveniently selected. For example,

$$\zeta_m = (m-1)t_i/n \tag{10}$$

will imply n equal intervals through the thickness of a layer.

The next task is comprised of supplying the $2N(n+1)$ equations for determination of as many unknown coefficients, $\bar{f}_{rm}^{(i)}$; $r = \alpha, \beta$; $i = 1, \ldots, N$; $m = 1, \ldots, n+1$. In what follows, first a strategy for obtaining the "exact" solution to the problem posed in this section will be discussed. Subsequently, three progressively approximate solution techniques will be described.

3. STRATEGY FOR "EXACT" SOLUTION

The present method supplies the aforementioned $2N(n+1)$ equations by (i) forcing σ_{rz}, $r = \alpha, \beta$ to vanish on the top and bottom surfaces of the laminated shell (four equations); (ii) satisfying continuity of σ_{rz} at each layer interface $\{2(N-1)$ equations$\}$; (iii) identifying $\bar{e}_{r\zeta}^{(i)}$, computed by the LCST-based finite element [eqn (1) of Chaudhuri and Seide, 1987a], as the physical components of transverse shear strains, which correspond to the through-the-thickness-average covariant components of the same ($2N$ equations); (iv) computation of jump in $\sigma_{rz,z}$ at each interface utilizing the first two equations of equilibrium of elasticity $\{2(N-1)$ equations$\}$; and finally (v) satisfying the first two equations of equilibrium of elasticity at $n-2$ points inside each layer $\{2N(n-2)$ equations$\}$.

Conditions (i) and (ii) above imply

$$\bar{f}_{r1}^{(1)} = \bar{f}_{r,n+1}^{(N)} = 0 \tag{11}$$

$$\bar{f}_{r1}^{(i)} = \bar{f}_{r,n+1}^{(i-1)} \tag{12}$$

for $r = \alpha, \beta$ and $i = 2, \ldots, N$.

Condition (iii) yields

$$(\gamma_{\alpha\zeta}^{(i)})_{av} = (\bar{\gamma}_{\alpha\zeta}^{(i)})_{FEM/LCST} \tag{13}$$

where

$$(\gamma_{\alpha\zeta}^{(i)})_{av} = \frac{1}{t_i}\int_0^{t_i} \gamma_{\alpha\zeta}^{(i)}(\zeta)\,d\zeta = \frac{\bar{g}_\alpha}{t_i}\int_0^{t_i}\left(1+\frac{\bar{d}_i+\zeta}{R_\alpha}\right)\varepsilon_{\alpha\zeta}^{(i)}(\zeta)\,d\zeta \tag{14a}$$

with

$$\varepsilon_{\alpha\zeta}^{(i)}(\zeta) = R_{44}^{(i)}\sigma_{\alpha\zeta}^{(i)}(\zeta) + R_{45}^{(i)}\sigma_{\beta\zeta}^{(i)}(\zeta) \tag{14b}$$

and

$$(\bar{\gamma}_{\alpha\zeta}^{(i)})_{FEM/LCST} = (\bar{\varepsilon}_{\alpha\zeta}^{(i)}(\zeta))_{FEM/LCST}\bar{g}_\alpha\left(1+\frac{\bar{d}_i+\zeta}{R_\alpha}\right). \tag{14c}$$

The assumed $\sigma_{\alpha\zeta}^{(i)}(\zeta)$, and $\sigma_{\beta\zeta}^{(i)}(\zeta)$, given by eqn (9), are then substituted in eqn (14b). An analogous set of equations can be obtained by setting $[\gamma_{\beta\zeta}^{(i)}]_{av}$ equal to $(\bar{\gamma}_{\beta\zeta}^{(i)})_{FEM/LCST}$.

Condition (iv) supplies another $2(N-1)$ equations by equating the jump in $\sigma_{rz,z}$, $r = \alpha, \beta$, at each interface computed using eqn (9) to that obtained utilizing the equation of equilibrium.

The jump in $\sigma_{\alpha z,z}$ at the ith interface is given by

$$\frac{\partial\sigma_{\alpha\zeta}^{(i+1)}(0)}{\partial\zeta} - \frac{\partial\sigma_{\alpha\zeta}^{(i)}(t_i)}{\partial\zeta} = \sum_{m=1}^{n+1}\left\{\bar{f}_{\alpha m}^{(i+1)}\frac{\partial H_m(0)}{\partial\zeta} - \bar{f}_{\alpha m}^{(i)}\frac{\partial H_m(t_i)}{\partial\zeta}\right\} = J_\alpha^{(i+1)} \tag{15a}$$

where $J_\alpha^{(i+1)}$ is obtained from the equation of equilibrium of elasticity, eqn (6a), in the form:

$$\begin{aligned} J_\alpha^{(i+1)} = \frac{-1}{\bar{g}_\alpha\bar{g}_\beta\left(1+\frac{\bar{d}_i+\zeta}{R_\alpha}\right)^2\left(1+\frac{\bar{d}_i+\zeta}{R_\beta}\right)}\Bigg\langle \frac{1}{\bar{g}_\alpha}\frac{\partial}{\partial\beta}\Bigg[\bar{g}_\alpha^2\left(1+\frac{\bar{d}_{i+1}}{R_\alpha}\right)^2\{\sigma_{\alpha\beta}^{(i+1)}(0) \\ -\sigma_{\alpha\beta}^{(i)}(t_i)\}\Bigg] + \bar{g}_\beta\left(1+\frac{\bar{d}_{i+1}}{R_\alpha}\right)\left(1+\frac{\bar{d}_{i+1}}{R_\beta}\right)\frac{\partial}{\partial\alpha}\{\sigma_\alpha^{(i+1)}(0)-\sigma_\alpha^{(i)}(t_i)\} \\ + \frac{\partial\bar{g}_\beta}{\partial\alpha}\left(1+\frac{\bar{d}_{i+1}}{R_\alpha}\right)^2\{\sigma_\alpha^{(i+1)}(0)-\sigma_\alpha^{(i)}(t_i)-\sigma_\beta^{(i+1)}(0)+\sigma_\beta^{(i)}(t_i)\}\Bigg\rangle \end{aligned} \tag{15b}$$

for $i = 1,\ldots,N-1$.

It is noteworthy that the right-hand side of eqn (15b) is comprised of the surface-parallel stresses and their derivatives with respect to the surface-parallel coordinates alone. $J_\beta^{(i+1)}$, the jump in $\sigma_{\beta z,z}$, can be obtained from the second equation of equilibrium of elasticity in a similar manner.

The remaining $2N(n-2)$ equations are supplied by condition (v), which is concerned with the satisfaction of the first two equations of equilibrium of elasticity at $n-2$ interior points ζ_k, $k = 1,\ldots,n-2$, of each layer. For example, substitution of eqn (9) into the left-hand side of the first equation of equilibrium of elasticity [eqn (6a)] will yield

$$\begin{aligned} \left\{\frac{2}{R_\alpha}\left(1+\frac{\bar{d}_i+\zeta_k}{R_\beta}\right)+\frac{1}{R_\beta}\left(1+\frac{\bar{d}_i+\zeta_k}{R_\alpha}\right)\right\}\left\{\sum_{m=1}^{n+1}\bar{f}_{\alpha m}^{(i)}H_m(\zeta_k)\right\} \\ +\left(1+\frac{\bar{d}_i+\zeta_k}{R_\alpha}\right)\left(1+\frac{\bar{d}_i+\zeta_k}{R_\beta}\right)\left\{\sum_{m=1}^{n+1}\bar{f}_{\alpha m}^{(i)}\frac{\partial H_m}{\partial\zeta}(\zeta_k)\right\} = F_i(\alpha,\beta,\zeta_k) \end{aligned} \tag{16}$$

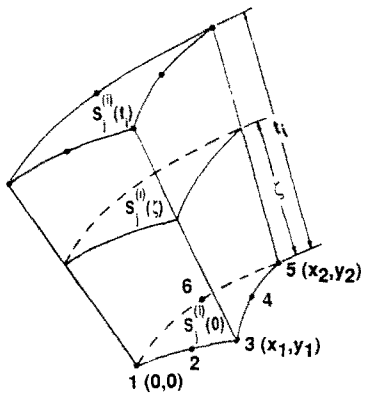

Fig. 1. The jth triangular layer-element belonging to the ith layer of a laminated shell.

for $k = 1, \ldots, n-2$; $i = 1, \ldots, N$; where $F_i(\alpha, \beta, \zeta_k)$ is obtained by substituting the surface-parallel stresses and their derivatives (with respect to α and β) obtained from the LCST-based finite element into the right-hand side of eqn (6a) at $n-2$ points ζ_k, $k = 1, \ldots, n-2$.

The second equation of equilibrium of elasticity provides a similar set of $N(n-2)$ equations in terms of $\bar{f}_{\beta m}(i)$.

4. APPROXIMATE TECHNIQUES

4.1. *Fixed natural coordinates basis vectors approximation*

The natural coordinate basis vectors, defined by Park and Stanley (1986) as

$$\mathbf{a}_r \sim \mathbf{g}_r/(g_{rr})^{1/2}, \quad r = 1,2 \text{ (no sum on } r) \tag{17a}$$

where

$$\mathbf{g}_r = \frac{\partial x^m}{\partial \theta^r}\mathbf{i}_m, \quad m, r = 1,2,3, \tag{17b}$$

can be assumed to be fixed when subjected to differentiation with respect to $\theta^1 = \alpha$, $\theta^2 = \beta$. This implies that for a sufficiently small element, which is reasonable to expect at the time of convergence,

$$\mathbf{g}_r \sim (g_{rr})^{1/2}\mathbf{a}_r \sim (g_{rr})^{1/2}\mathbf{i}_r, \quad r = 1,2,3 \text{ (no sum on } r). \tag{18}$$

This approximation will help simplify eqns (15) and (16) in the following manner. Computation of the various derivatives of the surface-parallel components of stresses with respect to α and β, which appear in eqns (15) and (16), will involve additional computations and also a slower rate of convergence, when obtained using an assumed displacement FEM. The appearance of these derivatives into the aforementioned two sets of equations is avoided by integration of both sides of eqn (1) over the volume of a triangular layer-element (Fig. 1) and then application of the divergence (Green–Gauss) theorem, as has been illustrated by Chaudhuri and Seide (1987a). This procedure, in conjunction with the assumption given by eqn (18), yields approximate forms of the first two equations of equilibrium of elasticity. For example, the first equation of equilibrium reduces to

$$\int\int_{\bar{s}_j} \sigma_{\alpha\zeta}^{(i)}(\zeta)\left(1+\frac{\bar{d}_i+\zeta}{R_\alpha}\right)\left(1+\frac{\bar{d}_i+\zeta}{R_\beta}\right)\mathrm{d}\bar{s} = \int\int_{\bar{s}_j} \sigma_{\alpha\zeta}^{(i)}(0)\left(1+\frac{\bar{d}_i}{R_\alpha}\right)\left(1+\frac{\bar{d}_i}{R_\beta}\right)\mathrm{d}\bar{s}$$
$$-\int_{\Gamma_j}\int_{\zeta}\{\sigma_\alpha^{(i)}(\zeta)\bar{n}_1+\sigma_{\alpha\beta}^{(i)}(\zeta)\bar{n}_2\}\left\{\left(1+\frac{\bar{d}_i+\zeta}{R_\Gamma}\right)^2+\left(\frac{\bar{d}_i+\zeta}{R_{n\Gamma}}\right)^2\right\}^{1/2}\mathrm{d}\zeta\,\mathrm{d}\Gamma \tag{19}$$

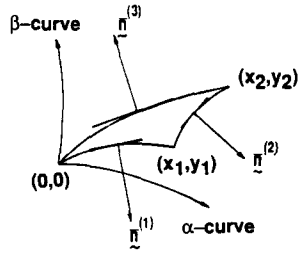

Fig. 2. A typical curved element interface.

where $\bar{s}_j$ and $\bar{\Gamma}_j$ are the area and perimeter, respectively, of the jth triangular element over the reference (bottom) surface of the laminated shell and $1/R_\Gamma$, $1/R_n$ are given by

$$\frac{1}{R_\Gamma} = \frac{\sin^2\bar{\phi}}{R_\alpha} + \frac{\cos^2\bar{\phi}}{R_\beta}$$

$$\frac{1}{R_{n\Gamma}} = -\left(\frac{1}{R_\alpha} - \frac{1}{R_\beta}\right)\sin\bar{\phi}\cos\bar{\phi}. \tag{20}$$

$\bar{n}_1$ and $\bar{n}_2$ at a point on each side of the curved triangle over the reference surface can be obtained in a manner discussed in the Appendix (also refer to Fig. 2).

For a flat plate, $R_\alpha = R_\beta = \infty$ and $g_\alpha = g_\beta = 1$, when rectangular Cartesian coordinates are used, i.e. $\alpha = x$, $\beta = y$. It has been shown by Chaudhuri (1986) and Chaudhuri and Seide (1987b) that for such a case $\sigma^{(i)}_{\alpha\zeta}(\zeta)$ averaged over the area of the element, $\bar{s}_j$, represents the exact transverse shear stress at the centroid of the interface triangle. For a laminated general shell, this is no longer deemed possible, because of the complexities introduced by g_α, g_β, R_α and R_β, which are, in general, complicated functions of α and β. However, a reasonably good estimate of $\sigma^{(i)}_{\alpha\zeta}(\zeta)$ [and $\sigma^{(i)}_{\beta\zeta}(\zeta)$] may be obtained by evaluating the surface integral as

$$\int\int_{\bar{s}_j} \sigma^{(i)}_{\alpha\zeta}(\zeta)\left(1+\frac{\bar{d}_i+\zeta}{R_\alpha}\right)\left(1+\frac{\bar{d}_i+\zeta}{R_\beta}\right)\mathrm{d}\bar{s} \sim \sigma^{(i)}_{\alpha\zeta}(\zeta)\left(1+\frac{\bar{d}_i+\zeta}{R_\alpha}\right)\left(1+\frac{\bar{d}_i+\zeta}{R_\beta}\right)\bar{s}_j. \tag{21}$$

The jump condition for $\sigma^{(i)}_{\alpha\zeta}(\zeta)$ is then given by eqn (15a) whose right-hand side can be expressed as

$$J^{(i+1)}_\alpha = \frac{-1}{\left(1+\frac{\bar{d}_{i+1}}{R_\alpha}\right)\left(1+\frac{\bar{d}_{i+1}}{R_\beta}\right)\bar{s}_j}\int_{\bar{\Gamma}_j}\left[\{\sigma^{(i+1)}_\alpha(0)-\sigma^{(i)}_\alpha(t_i)\}\bar{n}_1\right.$$

$$\left.+\{\sigma^{(i+1)}_{\alpha\beta}(0)-\sigma^{(i)}_{\alpha\beta}(t_i)\}\bar{n}_2\right]\left[\left(1+\frac{\bar{d}_{i+1}}{R_\Gamma}\right)^2+\left(\frac{\bar{d}_{i+1}}{R_{n\Gamma}}\right)^2\right]^{1/2}\mathrm{d}\Gamma \tag{22}$$

for $i = 1,\ldots,N-1$. $J^{(i+1)}_\beta$, $i = 1,\ldots,N-1$, can be obtained in a similar manner.

Finally, under the assumptions (approximations) embodied by eqns (18) and (19), condition (v) will yield a set of $N(n-2)$ equations for each of $\sigma^{(i)}_{\alpha\zeta}(\zeta)$ and $\sigma^{(i)}_{\beta\zeta}(\zeta)$, $i = 1,\ldots,N$. The set of $N(n-2)$ equations involving $\sigma^{(i)}_{\alpha\zeta}(\zeta)$ and the modified first equation of equilibrium is still given by eqn (16), the right-hand side of which, using eqn (20), can now be written as

$$F_i(\alpha,\beta,\zeta_k) = -\frac{1}{\bar{s}_j}\int_{\bar{\Gamma}_j}\{\sigma^{(i)}_\alpha(\zeta_k)\bar{n}_1+\sigma^{(i)}_{\alpha\beta}(\zeta_k)\bar{n}_2\}\left\{\left(1+\frac{\bar{d}_i+\zeta_k}{R_\Gamma}\right)^2+\left(\frac{\bar{d}_i+\zeta_k}{R_{n\Gamma}}\right)^2\right\}^{1/2}\mathrm{d}\Gamma. \tag{23}$$

A similar set of equations involving $\sigma_{\beta\zeta}^{(i)}(\zeta)$ can be obtained from the above situation by replacing the subscripts α by β and vice versa.

$\sigma_{\alpha\zeta}^{(i)}(\zeta)$ and $\sigma_{\beta\zeta}^{(i)}(\zeta)$ thus computed will represent the average transverse shear stresses over the area (on the reference surface) of the curved triangular element. This will yield reasonably accurate results, because the areas of the element become smaller and smaller as the convergence of displacements and stresses is approached. For numerical evaluation of the line integral, depending on the shell geometry, a sufficient number of points may be selected on each of the three sides of the curved element on the reference surface. This is illustrated in the case of flat plates and cylindrical and spherical shells by Chaudhuri (1983) and will not be reproduced here in the interest of the brevity of presentation. Computer implementation of the method for laminated general shells is currently underway at the University of Utah, the outcome of which will be published in a future paper. The present study will henceforth address the further approximate solutions of the problem, with an eye to achieving computational efficiency without sacrificing accuracy.

4.2. *Shallow shell approximation*

The next in line is the shallow shell approximation, which is frequently employed in obtaining analytical and numerical solutions for homogeneous and laminate shells. In the context of the present study, which uses the LCST-based FEM as the starting point, such an approximation will imply

$$\frac{\bar{d}_i+\zeta}{R_\alpha}, \frac{\bar{d}_i+\zeta}{R_\beta} \ll 1.$$

$\sigma_{r\zeta}^{(i)}(\zeta)$ may now be assumed to be in the form

$$\sigma_{r\zeta}^{(i)} = \sum_{m=1}^{3} \bar{f}_{rm}^{(i)} H_m(\zeta) \quad \text{for} \quad r = \alpha, \beta \tag{24}$$

where $H_m(\zeta)$ are the same as those for plates and given in Chaudhuri and Seide (1987b), which will imply that the prediction of distribution of each of the two interlaminar shear stresses through the thickness of an N-layer laminated shell will necessitate the determination of $3N$ unknown coefficients, which, in turn, ask for as many conditions or equations. These equations are now supplied by conditions (i)–(iv) mentioned earlier, while condition (v) is no longer required. It is noteworthy that the shallow-shell approximation renders the variation of the transverse shear stresses through the thickness of each layer parabolic, which is true for a flat plate under the hypothesis of the LCST. The details are available in Chaudhuri (1983, 1988) and will not be reproduced here in the interest of brevity.

4.3. *Cartesian-like local Riemann coordinates (CLRC) approximation*

Every Riemann space admits Riemann coordinates for any given origin, where all the Christoffel symbols vanish. The Riemann coordinates with origin in the present context may be defined as

$$x = \int_0^\alpha g_\alpha \, \mathrm{d}\alpha \quad \text{and} \quad y = \int_0^\beta g_\beta \, \mathrm{d}\beta \tag{25}$$

where x and y measure the (shortest) geodesic distance between any point (α, β) or (x, y) within the element and the local (element) origin along the α and β lines of curvature. These Riemann coordinates may be thought to behave like rectangular Cartesian coordinates in the vicinity of the local origin, because every Riemann space is also locally Euclidean (i.e. admits rectangular Cartesian coordinates), which implies that every sufficiently small (infinitesimally small in the limit) portion of the Riemann space is Euclidean. The above two concepts, Riemann coordinates with origin and Riemann space being locally Euclidean,

may be fused into one powerful approximation in the context of FEM (Chaudhuri and Seide, 1987a), which, when applied to the laminated shell analysis presented in Subsection 4.1, will simplify it to a level, obtainable in the case of a flat plate, presented in Chaudhuri and Seide (1987b), while retaining the curvature effect to a considerable extent. Further details are available in Chaudhuri (1983, 1988) and will not be reproduced here.

5. NUMERICAL RESULTS AND DISCUSSIONS

Numerical results for interlaminar shear stress distribution through the thickness of a laminated shell will be presented here. As a first step, these have been obtained using the CLRC approximation discussed earlier. Before studying a thick asymmetrically laminated shell, the present theory has first been tested for a thin homogeneous isotopic cylindrical shell, for which (reasonably accurate) numerical results, based on equilibrium method (henceforth, will be referred to as EM) and CLT-based closed-form solutions are available in Chaudhuri (1983) and Chaudhuri and Seide (1987a). The numerical results, obtained using the present theory, are very close to those due to the other two, which will not be repeated here in the interest of brevity. Instead, the following example problem will be investigated in detail.

Example: simply-supported asymmetrically laminated thick circular cylindrical shells under uniform internal pressure

A problem which illustrates the effect of lamination in a fibrous composite shell, is that of a pressurized two-layer, circular cylindrical shell, which is supported at both ends in such a way that only the radial deflection and the circumferential rotation are restrained, but the longitudinal rotation, the longitudinal displacement and the circumferential displacement are free to occur, i.e. SS1-type boundary condition (Hoff and Rehfield, 1965). The length and the inner radius of the shell are 20 in. and 10 in., respectively. The fiber-reinforced layers are identical except that the inner layer has a fiber orientation in the longitudinal direction while the fiber orientation in the outer layer, θ_2, varies. The elastic properties of a unidirectional (0°) lamina are assumed to be the same as those used by Spilker *et al.* (1977). E_{11} and E_{22} of the orthotropic layer material are 40×10^6 and 10^6 psi, respectively, while the shear moduli G_{12}, G_{13}, G_{23} are all assumed to be 0.5×10^6 psi. The major surface-parallel Poisson's ratio, ν_{12}, is taken to be equal to 0.25. The major transverse Poisson's ratios, ν_{13}, ν_{23}, are assumed to be the same. The displacements and stresses are independent of the circumferential coordinate, θ, but there is an additional rigid body rotation of the shell cross-sections. A closed-form solution for the problem with transverse shear deformation neglected is given by Chaudhuri *et al.* (1986). The convergence results of the displacements, the surface-parallel stresses and also the interlaminar shear stresses, computed using the aforementioned triangular shell element, are also available (Chaudhuri, 1983; Seide and Chaudhuri, 1987) and will not be repeated here.

The finite element model selected here is the same as has been utilized in the case of the EM (Chaudhuri and Seide, 1987a) and is shown in Fig. 3. First, the results using the CLRC approximation of the present FEM-based theory are computed for a thin laminated shell ($t = 0.2$ in.) and are compared with their counterparts, computed using the FEM-based equilibrium method of Chaudhuri and Seide (1987a) which utilized the same approximation, and also the CLT-based closed-form solution of Chaudhuri *et al.* (1986). Figure 4 shows the variation of σ_{xz} through the thickness of two-layer thin cylindrical shells for $\theta_2 = 0°$, 15°, 45° and 90° with $\theta_1 = 0°$. It is noteworthy that for the $\theta_2 = 0°$ case, the three sets of results are identical, because of the absence of layer-to-layer variation in shear deformation. For the remaining cases, the first two sets of results are almost identical, except that σ_{xz} (or $\sigma_{\theta z}$), as computed by the EM, does not completely vanish at the outer surface as required; however, this error is negligible. The CLT-based results, on the contrary, are in slight disagreement with the aforementioned two sets of LCST-based results, because of the neglect of the transverse shear deformation by the CLT, which is not true any more. Further results demonstrating the high accuracy of the present theory in the prediction of the transverse shear stresses in thin shells and detailed discussions on them

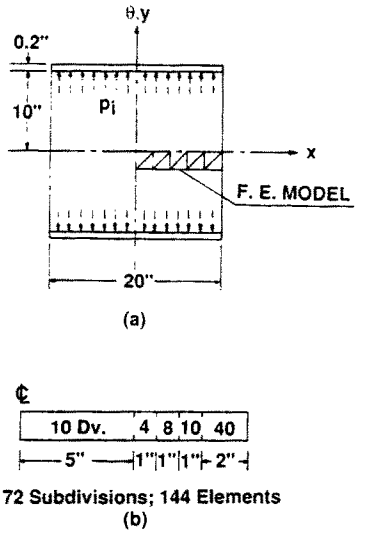

Fig. 3. (a) A circular cylindrical shell under internal pressure and (b) the finite element model.

are available in Chaudhuri (1983), and will not be reproduced here for the sake of brevity of presentation. In addition, the transverse shear stresses in three-layer symmetric (Chaudhuri, 1986) and two-layer unsymmetric (Chaudhuri and Seide, 1987b) plates can be reproduced by the present approach by considering arbitrarily large radius of the shell (e.g. $R = 10^5$ in.).

The primary focus of the present study is the presentation of hitherto unavailable numerical results for the interlaminar shear stresses and their through-thickness distributions in a thick asymmetrically laminated shell ($t = 5$ in.). Figure 5 presents the variation of σ_{xz}, at the end, $x = L/2$, through the thickness of the thick two-layer (0°/45°) tube. The results, obtained using the present approach and the CLRC approximation, are compared with their EM counterparts. As expected, σ_{xz}, as predicted by the EM, does not vanish on the outer surface. The success of the equilibrium method hinges on pointwise (in the three-dimensional sense) convergence of the second derivatives of the displacements. It is well known, however, that the first derivatives of the displacements, as computed by the assumed displacement FEM, converge in the mean-square sense (Strang and Fix, 1973), which will imply that in the case of an arbitrary laminated thick shell, the success of the EM is not guaranteed. The present solution is also compared with the closed-form solution, based on the CLT. The CLT overpredicts σ_{xz}, in the inner (0°) layer, except in a small region close to the interface, where the CLT underprediction is quite substantial. Figure 6 exhibits the variation of σ_{xz} over the half-length of the cylinder. The difference between the CLT prediction and that due to the present approach appears to be primarily due to the effect of the transverse shear deformation, which is neglected by the CLT; because, as has

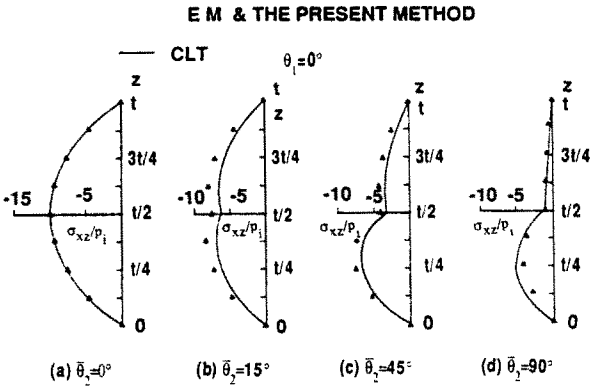

Fig. 4. Variation of σ_{xz} at the edge, $x = L/2$, through the thickness of a thin ($t = 0.2$ in.) 2-layer cylindrical shells.

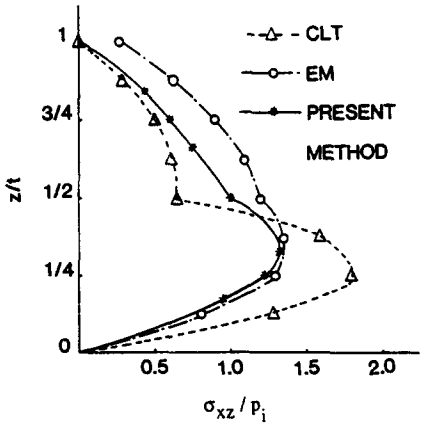

Fig. 5. Interlaminar shear stress distribution, at the edge, $x = L/2$ through the thickness of a thick ($t = 5$ in.) 0°/45° cylindrical shell.

been demonstrated in the preceding paragraph, the CLRC approximation, when employed judiciously, seems to be capable of yielding results of reasonably high accuracy.

6. CONCLUSIONS

A relatively "exact" (in the context of the problem posed in Section 2) and three progressively approximate semi-analytical methods for prediction of interlaminar shear stress distribution through the thickness of a thick arbitrarily laminated general shell have been presented. Even though the methods have been illustrated here for an assumed quadratic displacement triangular element, the principle behind them is general enough to be applicable for any element shape. Furthermore, this paper is the first to present the transverse shear stress distribution through the wall-thickness of a thick asymmetrically laminated shell. The Cartesian-like local Riemann coordinate (CLRC) approximation, which has been employed in obtaining the present results, gives a reasonably good estimate of the transverse shear stresses in an asymmetrically laminated thick shell. Results based on the more accurate theory and their comparisons with the three-dimensional elasticity solutions will be the topic of a future paper.

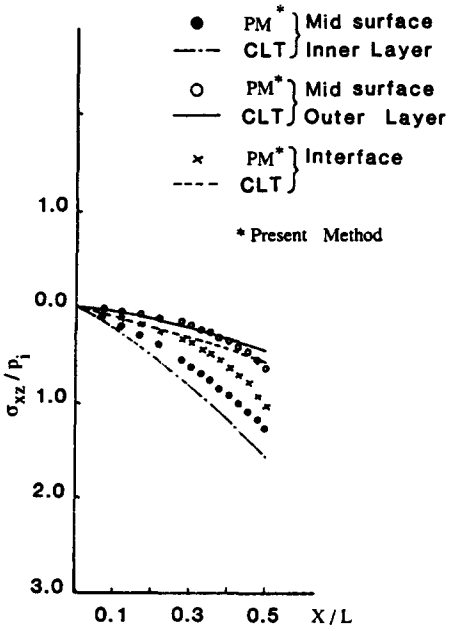

Fig. 6. Longitudinal variation of σ_{xz} for a thick ($t = 5$ in.) 0°/45° cylindrical shell.

REFERENCES

Chaudhuri, R. A. (1983). Static analysis of fiber reinforced laminated plates and shells with shear deformation using quadratic triangular elements. Ph.D. dissertation, Dept of Civil Engng., USC, Los Angeles.

Chaudhuri, R. A. (1986). An equilibrium method for prediction of transverse shear stresss in a thick laminated plate. *Comput. Struct.* **23**, 139

Chaudhuri, R. A. (1988). A semi-analytical approach for prediction of interlaminar shear stresses in a thick arbitrarily laminated anisotropic general shell. University of Utah Report.

Chaudhuri, R. A., Balaraman, K. and Kunukkasseril, V. X. (1986). Arbitrarily laminated anisotropic cylindrical shell under internal pressure. *AIAA Jl* **24**, 1851.

Chaudhuri, R. A. and Seide, P. (1987a). An approximate method for prediction of transverse shear stresses in a laminated shell. *Int. J. Solids Structures* **23**, 1145. Also the Errata (to be published).

Chaudhuri, R. A. and Seide, P. (1987b). An approximate semi-analytical method for prediction of interlaminar shear stress in an arbitrarily laminated thick plate. *Comput. Struct.* **25**, 627.

Hoff, N. J. and Rehfield, L. W. (1965). Buckling of axially compressed circular cylindrical shells at stresses smaller than the classical critical value. *J. Appl. Mech.* **32**, 542.

Park, K. C. and Stanley, G. M. (1986). A curved C shell element based on assumed natural-coordinate strains. *J. Appl. Mech.* **53**, 278.

Seide, P. and Chaudhuri, R. A. (1987). Triangular finite element for analysis of thick laminated shells. *Int. J. Num. Meth. Engng* **24**, 1563.

Spilker, R. L., Chou, S. C. and Orringer, O. (1977). Alternate hybrid-stress elements for analysis of multi-layer composite plates. *J. Compos. Mater.* **11**, 51.

Strang, G. and Fix, G. J. (1973). *An Analysis of the Finite Element Method.* Prentice-Hall, Englewood Cliffs, New Jersey.

Zienkiewicz, O. C. (1977). *The Finite Element Method*, 3rd Edn. McGraw-Hill, London.

APPENDIX

Let $\bar{n}_1$ and $\bar{n}_2$ referred to in eqn (19), at a point on the lth side of the interface triangle (Fig. 2), be denoted by $\bar{n}_r^{(l)}$, $l = 1, 2, 3$ and $r = 1, 2$, which can be determined for the element configuration shown in Fig. 2 in the following manner:

$$\begin{aligned}
\bar{n}_1^{(1)} &= (\bar{g}_{22})^{1/2}\frac{d\beta}{d\Gamma_{j1}} \\
\bar{n}_2^{(1)} &= -(\bar{g}_{11})^{1/2}\frac{d\alpha}{d\Gamma_{j1}} \\
\bar{n}_1^{(2)} &= (\bar{g}_{22})^{1/2}\frac{d\beta}{d\Gamma_{j2}} \\
\bar{n}_2^{(2)} &= -(\bar{g}_{11})^{1/2}\frac{d\alpha}{d\Gamma_{j2}} \\
\bar{n}_1^{(3)} &= -(\bar{g}_{22})^{1/2}\frac{d\beta}{d\Gamma_{j3}} \\
\bar{n}_2^{(3)} &= (\bar{g}_{11})^{1/2}\frac{d\alpha}{d\Gamma_{j3}}
\end{aligned} \tag{A1}$$

Computation of these quantities for specific shell geometries (e.g. cylindrical shell, spherical shell) is available in Chaudhuri (1983).